Clearance prediction of eight HIV protease inhibitors in man: role of hepatic uptake

Tom De Bruyn, Bruno Stieger, Patrick F. Augustijns and Pieter P. Annaert

Drug Delivery and Disposition, KU Leuven Department of Pharmaceutical and Pharmacological Sciences, O&N2, Herestraat 49 box 921, 3000 Leuven, Belgium (TDB, PFA, PPA)

Department Clinical Pharmacology and Toxicology, University Hospital, Zürich, Switzerland (BS)

Running title: Clearance of HIV protease inhibitors in man

Corresponding Author:

Pieter Annaert, PhD

Corresponding Author:

Pieter Annaert, PhD
Drug Delivery and Disposition
KU Leuven Department of Pharmaceutical and Pharmacological Sciences
O&N2, Herestraat 49 – box 921
B-3000 Leuven, Belgium.
Tel: 32-16-330303
Fax: 32-16-330305
E-mail: pieter.annaert@pharm.kuleuven.be

List of non-standard abbreviations:

APV, amprenavir; ATZ, atazanavir; CHO, Chinese hamster ovary; Cl, clearance; DMEM, Dulbecco's modified eagle medium; DRV, darunavir; FBS, fetal bovine serum; ES, estrone-3-sulfate; HEPES, 4-(2-hydroxyethyl)-1-piperazine ethanesulfonic acid; HIV, Human immunodeficiency virus; IDV, indinavir; LPV, lopinavir; NLV, nelfinavir; OATP/Oatp, Organic Anion Transporting Polypeptide (Human/Rat); OCT/Oct, Organic Cation Transporter (Human/Rat); PI, protease inhibitors; PBS, phosphate buffered saline; RAF, relative activity factor; RTV, ritonavir; SLC, Solute-linked carrier; SQV, saquinavir.

ABSTRACT

The aim of this work was to explore the contribution of the Organic Anion Transporting Polypeptide-1B (OATP1B) drug transporters in the hepatic clearance (Cl) of all marketed HIV protease inhibitors (PI) in humans. HIV PI uptake rates in OATP1B1/1B3-transfected CHO cells were converted to uptake Cl values in human hepatocytes a relative activity factor, which was determined by comparing uptake of known substrates between OATP1B1/3-transfected cells and human hepatocytes. Metabolic Cl values were determined in human liver microsomes. *In vivo* hepatic Cl values were calculated either by combining drug uptake and metabolism or based on one of these individual Cl processes and compared with published *in vivo* hepatic Cl values. Excellent *in vitro-in vivo* correlation ($R^2 = 0.85$) was observed when only uptake Cl values were used, but not when only metabolic Cl was used ($R^2 = 0.40$). The correlation did not improve when both processes were taken into account ($R^2 = 0.85$). PBPK models confirmed the remarkable sensitivity of predicted exposure to hepatic drug uptake, indicating a key role for OATP1B1/3 in hepatic disposition of several HIV PI in man. This may contribute to the inter-individual variability in systemic and hepatic exposure to these drugs in the clinic.

INTRODUCTION

Over the last decades, hepatic uptake transporters have been recognized to play a determining role in the hepatic disposition of many endogenous and exogenous compounds. In particular, members of the organic anion transporting polypeptide family (OATP; *SLCO* gene family) influence the hepatic Cl of many drugs. The most important members of the OATP family in the basolateral membrane of the hepatocyte are the hOATP1B1 (*SLCO1B1*) and hOATP1B3 (*SLCO1B3*) isoforms.[1] Genetic polymorphism as well as inhibition or induction of OATP activity can lead to altered plasma concentrations and clinically important drug-drug interactions.[2–4]

HIV PI represent an important class of therapeutic agents in the currently recommended treatment (Highly Active Antiretroviral Therapy; HAART) of HIV infection. Among the HIV PI that have been approved, lopinavir, atazanavir, darunavir and fosamprenavir are most frequently prescribed.[5,6] HIV PI are extensively metabolized by CYP3A enzymes [7,8] and their biliary excretion is mediated by the efflux transporters P-gp (*ABCB1*) and MRP2 (*ABCC2*).[8,9] In addition, it has been shown that some HIV PI (or their metabolites) are excreted via the feces for more than 75 %.[8] This illustrates that hepatic elimination is much more important than renal elimination for these drugs.

Based on experiments with clinically relevant concentrations of nelfinavir, ritonavir and saquinavir in suspended rat hepatocytes, Parker and Houston reported that hepatic uptake rather than metabolism is the rate-limiting factor in the hepatic disposition of these compounds.[10] Moreover, in addition to a carrier-mediated process, passive transmembrane permeation significantly contributed to the hepatic uptake of saquinavir and ritonavir.[11] In general, previous results imply that a carrier-mediated process is

involved in the hepatic uptake of HIV PI. It follows that the 'interplay' between transport and metabolism has to be considered for these compounds.[12,13]

Several studies have illustrated that HIV PI inhibit the *in vitro* cellular uptake of OATP1B probe substrates like estradiol-17β-D-glucuronide, CGamF and sodium fluorescein.[14–17] Moreover, it has been suggested that inhibition of these membrane transporters contributes to clinically important antiretroviral drug-drug interactions, for example with cerivastatin and atorvastatin.[18] While these examples certainly illustrate the clinical relevance of OATP modulation by HIV PI, the concept of meaningful OATP-mediated transport of HIV PI remains controversial. Current evidence in this respect includes OATP1A2-mediated transport of saquinavir in HepG2 cells.[19] Consistently, Hartkoorn et al. showed that saquinavir, darunavir and lopinavir have affinity for both OATP1A2 and OATP1B1 and that saquinavir is also transported by OATP1B3.[20] Furthermore, it has been shown that the single nucleotide polymorphism 521T>C in *SLCO1B1* is associated with significantly increased plasma concentrations of lopinavir.[20,21] In contrast, a recent publication showed that the hepatic uptake of nelfinavir, lopinavir and ritonavir is primarily mediated by passive diffusion in sandwich-cultured human hepatocytes.[22] Additionally, they suggested an unidentified sinusoidal uptake transporter for amprenavir. These conflicting findings highlight the need for further exploration of the exact role of transporter-mediated hepatic uptake of HIV PI in their disposition profiles. Therefore, this study aimed to investigate the contribution of hepatic uptake for all marketed HIV PI in one study under equal conditions. To achieve this goal, *in vitro* data for uptake and/or metabolism were extrapolated to *in vivo* hepatic Cl values and retrospectively compared with published non-renal Cl values.

MATERIALS AND METHODS

Chemicals. Ritonavir, indinavir sulfate, saquinavir mesylate, nelfinavir mesylate were obtained from Hetero Drugs Limited (Hyderabad, India). Amprenavir was kindly donated by GlaxoSmithKline (Middlesex, UK). Atazanavir was provided by Bristol-Myers Squibb (New Brunswick, NJ) and darunavir, lopinavir and tipranavir were obtained through the NIH AIDS Reagent Program. Dulbecco's modified eagle medium (DMEM), Hanks' balanced salt solution (HBSS), L-glutamine, fetal bovine serum (FBS), penicillin-streptomycin mixture (contains 10,000 IU potassium penicillin and 10,000 µg streptomycin sulfate per ml in 0.85% saline) and Trypsin EDTA were purchased from Lonza SPRL (Verviers, Belgium). Geneticin G418 was purchased from Invitrogen (Paisley, UK). HEPES [4-(2- hydroxyethyl)-1-piperazine-ethanesulfonic acid] was purchased from MP Biochemical (Illkirch, France). Triton X-100, bovine serum albumin, sodium fluorescein, L-proline and sodium butyrate were purchased from Sigma-Aldrich (Schnelldorf, Germany). For uptake experiments with suspended human hepatocytes, cryopreserved human hepatocytes were re-suspended in Krebs-Henseleit Buffer (NaCl 130 mM, KCl 5.17 mM, $CaCl_2$ 1.2 mM, $MgCl_2$ 1.2 mM, HEPES 12.5 mM, Glucose 11.1 mM, Na-pyruvate 5 mM; pH 7.4).

Culture of OATP-transfected CHO cells. Wild-type and OATP1B1- and OATP1B3-transfected CHO cells were cultured at passage 45 to 65, as described previously.[15] CHO cells were grown in 75 cm^2 T-Flasks in DMEM containing 1 g/l D-glucose, 1 mM L-glutamine, 25 mM HEPES and 110 mg/l sodium pyruvate, supplemented with 10 % FBS, 50 µg/ml L-proline, 100 IU/ml penicillin, 100 µg/ml streptomycin. The culture media of the transfected cell lines additionally contained 500 µg/ml geneticin. Cells were incubated

at 5% CO_2 and 37°C. For uptake experiments, wild-type CHO cells were seeded in 12-well cell culture plates (Greiner-Bio-One, Wemmel, Belgium) at a density of 20,000 cells/well while CHO-transfected cells were seeded at a density of 25,000 cells/well. Culture medium was replaced every other day and uptake experiments were performed on day 4-5 after seeding when cells were reaching confluency. One day before the experiment, both wild-type and transfected cells were additionally treated with 5 mM sodium butyrate to induce gene expression.

Uptake studies in transfected CHO cells. Uptake experiments in transfected CHO cells were performed as described previously.[15] Briefly, cells were washed twice with 1 ml/well pre-warmed uptake buffer (HBSS with 10 mM HEPES, pH 7.4) and pre-incubated for 5 min at 37 °C. After the pre-incubation, uptake buffer was aspirated and 1 ml/well of uptake buffer, containing the desired substrate concentration was added. Cells were incubated for 30 s at one clinically relevant test concentration, corresponding to the maximum *in vivo* unbound plasma concentrations (see Table 1). Consequently, medium was quickly aspirated and cells were rinsed three times with ice-cold uptake buffer. Cells were lysed with 0.3 ml/well of a 70/30 methanol/water mixture (or 0.5 % Triton X in PBS for CGamF and estrone-3-sulfate) and placed on a plate shaker for 30 min at room temperature. Cell lysates were transferred to a 1.5 ml microcentrifuge tube. Samples were stored at -20°C until analysis. For estrone-3-sulfate, a 200 µl sample was transferred to a scintillation vial containing 2 ml of scintillation cocktail and radioactivity was quantified using liquid scintillation spectrometry (Wallac 1410, Finland). For CGamF, fluorescence was measured using fluorescence spectroscopy (excitation/emission wavelength; 494/520 nm) in a Tecan Infinite M200 plate reader (Tecan Benelux, Mechelen, Belgium). Mean

protein content/well was determined by measuring protein content of three wells for each batch of CHO cells using a BCA Protein assay kit (Pierce Chemical, Rockford, IL).

Uptake studies in cryopreserved human hepatocytes. Cryopreserved human hepatocytes were provided by Life Technologies. (Invitrogen, Durham, NC). Uptake experiments in human hepatocytes were performed as described previously.[23] After thawing the hepatocytes at 37°C, cells were re-suspended in thawing medium (consisting of DMEM, 10 % (v/v) FBS, 100 IU/ml penicillin, 100 µg/ml streptomycin, 4 µg/ml insulin and 1 µM dexamethasone) and centrifuged at 168 *g* for 20 min. To wash the cells, the pellet was re-suspended in 15 ml of thawing medium and centrifuged at 50 *g* for 3 min. Subsequently, hepatocytes were re-suspended in uptake buffer and cell viability and yield were determined with the Trypan blue method. The cell suspension was further diluted with uptake buffer to a cell density of 2 million cells/ml (double-concentrated cell suspension) and kept on ice until the start of the uptake experiments. Before the incubation, the double-concentrated cell suspension (500 µl) was pre-incubated for 5 min at 37 °C. Subsequently, 500 µl of a pre-warmed double-concentrated CGamF solution (20 µM) was added to initiate the incubation. To determine the non-saturable uptake component, experiments were also conducted at 4°C. After an incubation period of 90 s, triplicate 200 µl aliquots of the suspension were transferred to 1.5 ml ice-cold microcentrifuge tubes, containing 700 µl of an oil layer (silicone / mineral oil mixture; density, 1.015) above 300 µl of 8 % NaCl solution. Subsequently, the tubes were immediately centrifuged for 3 min at 16,000 *g* using a tabletop centrifuge (Eppendorf 5415 C, Hamburg, Germany). After freezing microcentrifuge tubes in dry ice, the tube bottoms were cut and the contents solubilized in 300 µl 0.5% Triton X (in PBS). CGamF

concentration was measured by fluorescence spectroscopy (ex 494 nm; em 520 nm) in a Tecan Infinite M200 plate reader (Tecan Benelux, Mechelen, Belgium). Uptake rates were normalized for the cell density during the incubation and expressed as pmol/min/million cells.

***In vitro* metabolism studies in pooled human liver microsomes.** Pooled human liver microsomes (45 donors) were provided by Kaly-Cell (Plobsheim, France). Drug depletion experiments were performed in a total volume of 400 µl in 48-well culture plates (Greiner-Bio-One, Wemmel, Belgium) placed in a shaking incubator (350 rpm, 37°C). Microsomes were gently thawed at 37°C and diluted to a 4-fold concentrated protein concentration in microsomal incubation buffer (consisting of 3 mM MgCl2, 100 mM sodium phosphate buffer, pH 7.4). A double-concentrated substrate solution (200 µl) was pre-incubated with a 4 fold-concentrated suspension of human liver microsomes (100 µl) for 10 min. To initiate the depletion experiment, 100 µl of a pre-warmed solution of NADPH (4 mM) and glucose-6-phosphate (12 mM) was added. Samples (75 µl) were taken at different time points (0, 10, 20 and 30 min) and were added to an equal volume of ice-cold acetonitrile (containing the internal standard) to terminate the reaction. Samples were stored at -20°C until analysis.

Determination of unbound fraction in liver microsomes. The fraction unbound in microsomal medium fu_{mic} was determined by equilibrium dialysis performed with a HTDialysis apparatus (HTDialysis LLC, Gales Ferry, CT) and a dialysis membrane with a 12-14 kDa MW cutoff. Drug solutions (10 µM) were prepared in incubation medium containing 0.25 mg liver microsomal protein/ml and equilibrium dialysis was performed against protein-free microsomal incubation buffer in a shaking device (175 rpm) at 37°C.

Samples were taken from both sides of the well after 4 h and stored at -20°C until analysis. The fraction unbound was calculated as the ratio of drug concentration in the protein-free medium over that in the protein-containing medium.

LC-MS/MS analysis. Samples from experiments with transfected cells, liver microsomes and hepatocytes were vortexed and centrifuged at 10,000 *g* for 10 min. The supernatant was transferred to high performance liquid chromatography vials and analyzed by ultra-performance liquid chromatography tandem mass spectrometry. A Thermo Scientific (San Jose, CA) Accela pump, Accela autosampler, and a Waters Acquity CSH D18 column (3.0 x 50 mm, 1.7µm) with a VanGuard pre-column were used for all chromatographic separations. The mobile phase initially consisted of 95/5, v/v (0.5 mM ammonium acetate buffer, pH 3.5 / methanol), which gradually decreased to 5/95, v/v (0.5 mM ammonium acetate buffer, pH 3.5 / methanol) over 2 min. After 1 min, the initial condition of 95/5, v/v (0.5 mM ammonium acetate buffer, pH 3.5 / methanol) was again obtained (over 10 s) and maintained for 1 min. The flow rate was 400 µl/min. The column oven and autosampler temperature were set at 30° and 15 °C, respectively. Tandem mass spectrometry detection was carried out using a Thermo TSQ Quantum Access (Thermo Fisher Scientific, San Jose, CA) with an Ion Max H-ESI source in positive ionization mode. Transitions monitored and automatically optimized electric parameters are listed in Table 2. For all analytical methods, the intra- and interday precision (n = 6) of standards with low (5 nM), medium (50 nM) and high (500 nM) concentration was below 15 %, 10 % and 10 %, respectively. Both intra- and interday bias of the same standards was lower than 10 %.

Kinetic analysis. Net uptake values were obtained by subtracting uptake in wild-type CHO cells and uptake in hepatocytes at 4°C from total uptake at 37°C in transfected cells and hepatocytes, respectively. Subsequently, uptake Cl values (µl/min/mg protein or µl/min/million cells) were calculated by dividing the net uptake value by the corresponding substrate concentration.

Similarly, passive uptake Cl values were calculated by dividing uptake in wild-type CHO cells by the corresponding substrate concentration.

For drug depletion experiments, the log of the drug concentration was plotted in function of time and the elimination constant was calculated by fitting a single exponential decay. This elimination constant was used to calculate the half-life of the metabolic turn-over, which was further converted to the intrinsic metabolic Cl according to following equation:[24]

$$Cl_{int} = \left(\frac{0.693}{t_{1/2}} \times \frac{incubation\ volume}{\text{mg protein}} \right) \qquad \text{Eq.1}$$

These Cl values, determined for different substrate concentrations, were further converted to the metabolic rates by multiplying them with the corresponding substrate concentrations. Metabolic rate data in function of concentration followed Michaelis-Menten kinetics and non-linear regression in R for Windows (v. 2.15, R Foundation, Vienna, Austria) was used to determine the kinetic parameters K_m and V_{max}. The intrinsic metabolic Cl ($Cl_{int,met}$) was calculated as follows:

$$Cl_{int,met} = \frac{V_{max} \times \mathrm{C}}{K_m + (f_{u,mic} \times \mathrm{C})} \qquad \text{Eq.2}$$

Estimation of uptake Cl of HIV PI in human hepatocytes. The methodology based on relative activity factor (RAF) to estimate the contribution of each transporter to the total

hepatic uptake was introduced by Kouzuki et al. and applied to estimate the contribution of OATP1B1 and OATP1B3 to the hepatic uptake of fexofenadine, pitavastatin and rosuvastatin in humans.[25–28] Following this method, we derived the hepatic Cl of all HIV PI in human hepatocytes. With an OATP1B1/OATP1B3 uptake ratio of 9.14 for estrone-3-sulfate and 0.14 for CGamF, these probe substrates have been shown to be strongly preferred substrates of OATP1B1 and OATP1B3, respectively.[15] The ratio of the uptake Cl of these reference compounds in human hepatocytes to that in transfected CHO cells is defined as the relative activity factor (RAF) and was calculated as described in following equations:

$$RAF_{OATP1B1} = \frac{Cl_{\text{Hep, ES}}}{Cl_{\text{OATP1B1, ES}}} \quad \text{Eq. 4}$$

$$RAF_{OATP1B3} = \frac{Cl_{Hep,CGamF}}{Cl_{OATP1B3,CGamF}} \quad \text{Eq. 5}$$

Subsequently, the uptake Cl of all HIV PI in human hepatocytes $Cl_{int,upt}$ was calculated as the sum of the uptake Cl of HIV PI in transfected CHO cells multiplied by the corresponding RAF values, as described by following equation:

$$Cl_{int,upt} = Cl_{OATP1B1,HIV\ PI} \times RAF_{OATP1B1} + Cl_{OATP1B3,HIV\ PI} \times RAF_{OATP1B3} \quad \text{Eq. 6}$$

The passive uptake Cl of HIV PI in human hepatocytes was estimated based on the passive diffusion measured in wild-type CHO cells by correcting for the different cell surface area between human hepatocytes (1093 μm^2) and CHO cells (615 μm^2).[29,30] To anticipate the effects of potential differences in passive diffusion in CHO cells and human hepatocytes, we simulated the effect of passive uptake Cl on the relationship between reported and calculated hepatic Cl of HIV PI.

***In vitro – in vivo* extrapolation of hepatic Cl.** To evaluate the rate-limiting step in the overall hepatic elimination of HIV PI, the reported *in vivo* hepatic Cl of HIV PI was

predicted based on uptake data only, metabolism data only or a combination of both. Therefore, the determined *in vitro* intrinsic uptake or metabolic Cl values were first scaled to the intrinsic *in vivo* Cl by following reported scaling factors; hepatocytes per gram liver (HPGL) of 117.5, microsomal protein per gram liver (MPPGL) of 39.8 and a liver weight of 1648 g. Based on the well stirred model, these intrinsic *in vivo* Cl values were converted to hepatic Cl values according to following equations;

$$Cl_{Hep,upt} = \frac{Q_h \times f_u \times (Cl_{int,upt} + Cl_{passive})}{Q_h + f_u \times (Cl_{int,upt} + Cl_{passive})} \qquad \text{Eq. 7}$$

$$Cl_{Hep,met} = \frac{Q_h \times f_u \times Cl_{int,met}}{Q_h + f_u \times Cl_{int,met}} \qquad \text{Eq. 8}$$

with Q_h the *in vivo* hepatic plasma flow (900 ml/min) and f_u the reported unbound fraction in plasma (Table 1). To predict hepatic plasma Cl based on the combination of both uptake and metabolism data, following equation was used;[31]

$$Cl_{Hep} = \frac{Q_h \times f_u \times Cl_{int,met} \times (Cl_{int,upt} + Cl_{passive})}{Q_h \times (Cl_{int,met} + Cl_{passive}) + ((Cl_{int,upt} + Cl_{passive}) \times f_u \times Cl_{int,met})} \qquad \text{Eq. 9}$$

PBPK modelling for amprenavir, atazanavir and darunavir. Plasma concentration time profiles for three selected HIV protease inhibitors (amprenavir, darunavir, atazanavir) were predicted with the Simcyp simulator v14.1 (Certara, Princeton NJ). The relevant physicochemical data along with previously reported in vitro data on these model PI as well as in vitro hepatic disposition data generated in the present study are shown in Table 3. The distribution volume was predicted by modifying the scalar for tissue/plasma partition coefficients to obtain a value corresponding to the reported volume of distribution. A comparison was made with clinically observed systemic exposure profiles of these HIV PI following single oral dosing at relevant dose. Exposure

profiles were first predicted taking into account only hepatic enzyme kinetics (as determined in human liver microsomes in the present study). Subsequently, the permeability-limited liver model was applied by implementing values for passive (sinusoidal) transmembrane clearance as well as OATP1B1/3-mediated uptake clearances as measured in the present study. The values used for each HIV PI are also included in Table 3.

Statistics A two-tailed Student's t-test (analysis tool in Microsoft Excel 2010, $p < 0.05/0.01$) was used to evaluate statistical differences between uptake in wild-type and OATP1B1/OATP1B3-transfected CHO cells.

RESULTS

Time-dependent uptake of HIV PI.

Stably-transfected OATP1B1/3 CHO cells represent a validated *in vitro* model to study the contribution of a distinct transporter isoform in the hepatic disposition of a compound.[14,15,32] To mimic the dynamic *in vivo* environment in view of determining transport kinetics, initial uptake rates should be measured. Therefore, initial uptake experiments were performed as a function of time in order to determine the linear range in the *in vitro* profiles. Supplemental Figure 1 shows the time-dependent uptake of tipranavir (0.25 μM) and indinavir (2.5 μM) in wild-type and OATP1B1- and OATP1B3-transfected CHO cells, demonstrating that initial uptake rates in transfected CHO cells decrease at incubation times longer than 30 s, while in wild-type CHO cells, linearity is maintained up to 90 s. Comparable profiles were obtained for other HIV PI. In further experiments, a 30 s incubation time was employed (which also represents the first practically feasible time point).

Uptake of HIV PI in transfected CHO cells.

A systematic comparison of the uptake of all HIV PI in OATP1B1- and OATP1B3-transfected cells is shown in Figure 1. Cells were incubated for 30 s at one clinically relevant test concentration, corresponding to the maximum *in vivo* unbound plasma concentrations (see Table 1). In OATP1B1-transfected CHO cells, atazanavir and lopinavir showed the highest relative uptake (> 3 fold). Except for amprenavir (where the uptake was lower compared to wild-type cells), the uptake of other HIV PI was also significantly higher compared to wild-type CHO cells. In OATP1B3-transfected CHO cells, tipranavir showed the highest relative uptake (3-fold), whereas the uptake ratios of

darunavir, atazanavir, saquinavir, ritonavir and nelfinavir were comparable (1.5-2-fold). The uptake of lopinavir in OATP1B3-transfected cells was not significantly higher compared to the uptake in wild-type cells. Amprenavir showed lower uptake in both transfected cell lines than in wild-type CHO cells.

Estimation of the uptake Cl of HIV PI in human hepatocytes.

The uptake Cl of all HIV PI in human hepatocytes was estimated using the RAF approach, previously applied to estimate the Cl of pitavastatin, rosuvastatin and fexofenadine in human hepatocytes.[26–28]

The ratio between the uptake Cl of reference compounds (estrone-3-sulfate for OATP1B1 and CGamF for OATP1B3) determined in human hepatocytes and transfected cells, is defined as the relative activity factor (Table 4). These RAF values were used to predict the active uptake Cl of HIV PI in human hepatocytes (Table 5) as described in the materials and methods section. Calculated total uptake Cl values (as the sum of active and passive Cl) of HIV PI in human hepatocytes ranged from 12.1 to 383.4 μl/min/million cells.

Metabolic Cl of HIV PI in human liver microsomes.

Metabolic Cl of all HIV PI was determined using the half-life approach over a range of concentrations (0.1 – 5 μM) in pooled human liver microsomes (0.025-0.25 mg protein/ml). Depletion profiles were log-linear over the time-course studied (up to 30 min) with a minimum compound loss of 20 %. As illustrated for tipranavir in Figure 2, metabolic rate in function of concentration followed Michaelis-Menten type kinetics. The kinetic parameters Km, Vmax and Cl are summarized in Table 6 for all HIV PI. The

intrinsic metabolic Cl was corrected for the unbound fraction in the microsomal incubation medium fu_{mic} (Eq 2).

Hepatic Cl predictions of HIV PI.

The *in vitro* Cl values for hepatic uptake ($Cl_{int,upt}$ and $Cl_{passive}$) and metabolism ($Cl_{int,met}$) were scaled up and the hepatic plasma Cl was calculated based on the individual processes or on the combination of both uptake and metabolism according to equations 7, 8 and 9, respectively.

The relationship between the reported and calculated hepatic Cl of all HIV PI is shown in Figure 3. Based on uptake data only (Figure 3, panel A), a linear correlation ($R^2 = 0.85$) between the reported and predicted *in vivo* Cl was found, although *in vivo* hepatic Cl was systematically under-predicted by approximately a factor 4. In contrast, a poor correlation ($R^2 = 0.40$) was observed when *in vitro – in vivo* extrapolations were based on metabolism data only (Figure 3, panel B). When both uptake and metabolism processes were taken into account (Figure 3, panel C), the correlation between reported and predicted *in vivo* hepatic Cl was equal to that based on uptake data only ($R^2 = 0.85$).

The effect of the passive uptake Cl on the relationship between reported and calculated hepatic Cl values of HIV PI is shown in Figure 4. When the experimentally determined passive uptake Cl of each protease inhibitor was increased or decreased with a factor 2, a minimal effect on the correlation coefficient was observed. On the contrary, when passive uptake Cl becomes less than 40 % of the experimentally determined passive uptake Cl, a poor relationship is obtained between the reported and calculated hepatic Cl values of HIV PI.

Simulating the impact of modulation of transporter activity on clearance.

To simulate the interaction potential with active hepatic uptake of HIV PI, the effect of inhibition and induction of the hepatic uptake on the hepatic Cl of HIV PI is represented in Figure 5. This simulation showed that the hepatic Cl of atazanavir, lopinavir and tipranavir decreased approximately by 50 % when active hepatic uptake is inhibited by 90 %. On the contrary, a limited decrease of the hepatic Cl of other HIV PI is observed when active uptake was inhibited. The predicted effect of induction of transporter expression on the hepatic Cl of hepatocytes revealed a significant increase in the hepatic Cl of darunavir, atazanavir, lopinavir, ritonavir and tipranavir when hepatic uptake was 5 times increased, whereas only a limited effect was observed for nelfinavir, saquinavir, indinavir and amprenavir.

PBPK modelling for amprenavir, atazanavir and darunavir.

Predicted plasma concentration time profiles (Figure 6) based on PBPK models assuming perfusion-limited hepatic elimination ignore the possible role of active and passive hepatic uptake transport. Under those conditions, plasma concentrations are largely underpredicted (implying overprediction of hepatic clearance). When permeability-limited liver models are applied, the values obtained in the present study for passive uptake clearance as well as for OATP1B1 and OATP1B3-mediated uptake can be implemented. This resulted in a very good prediction of atazanavir exposure, whereas some improvement is observed for the other two HIV protease inhibitors.

DISCUSSION

HIV PI are potent inhibitors of the hepatic transport proteins OATP1B1 and OATP1B3.[14,16,17,33] Consistently, OATP inhibition explained the marked increase in the area under the plasma concentration-time curve of the OATP1B1 substrates bosentan and rosuvastatin, when co-administered with the combination of lopinavir and ritonavir in healthy volunteers.[34,35] In addition to the OATP1B inhibitory potential of HIV PI, several studies revealed that these drugs also show affinity for OATP1B isoforms as substrates.[19,20] Moreover, the 521T>C gene polymorphism in *SLCO1B1* is significantly associated with higher lopinavir plasma concentrations.[20] These findings raise the question whether hepatic OATP isoforms play a pivotal role in the hepatic uptake of HIV PI. The aim of this study was to further investigate the exact role of hepatic uptake transport in the overall hepatic Cl of HIV PI.

The uptake of HIV PI in OATP1B-transfected CHO cells (Figure 1) confirmed that lopinavir, darunavir and saquinavir are substrates for OATP1B1 and that saquinavir is also a substrate for OATP1B3 as published by Hartkoorn et al.[20] In addition, we showed that also other HIV PI including atazanavir, tipranavir and indinavir are transported by these uptake transport proteins. The relatively limited contribution of uptake transporters for nelfinavir and ritonavir is in agreement with a recent publication by Liu et al. in sandwich-cultured human hepatocytes. [22] The observation that amprenavir uptake is not enhanced in OATP1B-transfected cells is consistent with its relative low inhibitory capacity (higher *Ki* values) of the OATP1B probe substrates (e.g. sodium fluorescein) compared to other HIV PI.[14,15,17] Surprisingly, amprenavir uptake was lower in

transfected-CHO cells, which may explained by the action of endogenous (efflux) transporters in this model system.

Suspended or sandwich-cultured human hepatocytes are routinely used to determine the hepatic uptake Cl of drugs or drug candidates. Nevertheless, these *in vitro* model systems are characterized by the involvement of other processes determining the overall hepatic Cl (e.g. metabolism and biliary excretion) and often show high inter-donor variability in transporter activities.[23] Therefore, we estimated an average intrinsic uptake Cl of HIV PI in human hepatocytes based on transfected CHO cells by relying on relative activity factors (RAF).[26–28] The RAF, the ratio between the uptake Cl values of selective reference compounds in human hepatocytes and transfected cells, is used to extrapolate the uptake Cl of test compounds determined in transfected cells to the uptake Cl in human hepatocytes Cl (Table 5 and 6). Experimentally determined RAF values for estrone-3-sulfate (0.70, OATP1B1) and CGamF (0.1, OATP1B3) are in good agreement with those previously published for the OATP1B1 substrate estrone-3-sulfate (0.76) and the OATP1B3 substrate cholecystokinin octapeptide (0.16).[26] When intrinsic uptake Cl values were further extrapolated to the hepatic Cl with the well stirred model, a good correlation (R^2 = 0.85) between predicted and reported and *in vivo* Cl values was observed (Figure 3, panel A). This suggests that hepatic uptake is the rate-limiting process in the overall Cl of HIV PI.

To compare the relative role of hepatic uptake to that of metabolism, we also estimated the hepatic Cl of HIV PI based on metabolism data only. Previous research has shown that the *in vivo* hepatic Cl can accurately be estimated from *in vitro* data in both microsomes and hepatocytes.[36] Nevertheless, hepatic uptake transporters have been

shown to modulate Cl of compounds that is predominantly mediated by metabolic enzymes when measured in hepatocyte systems.[31] Therefore, the metabolic intrinsic Cl of HIV PI was measured in pooled liver microsomes (Table 6). In general, our metabolic data were consistent with previously published metabolic Cl values determined in human microsomes with a maximum 5-fold difference for darunavir.[37–40] This discrepancy as well as other small deviations from our data may result from differences in methodology or the lack of correction for nonspecific binding in some studies. When intrinsic metabolic Cl values were extrapolated to the hepatic Cl with the well stirred model, a poor correlation with the reported *in vivo* Cl values of HIV PI (R^2 = 0.40) was found (Figure 3, Panel B). This illustrates that even for drugs that are generally regarded as being extensively metabolized, hepatic uptake can still play a significant role in the overall hepatic Cl.

To further investigate the interplay between hepatic uptake and metabolism, the *in vitro – in vivo* extrapolation of the hepatic Cl of HIV PI was also conducted using a model, incorporating both hepatic uptake and metabolic Cl values.[31] Compared to the approach based on hepatic Cl only, no further improvement of the *in vitro – in vivo* correlation (R^2 = 0.85) was observed (Figure 3, Panel C), further confirming the rate-determining role of hepatic uptake in the overall Cl.

Because we estimated the passive Cl of HIV PI in human hepatocytes based on the passive diffusion into wild-type CHO cells, we also simulated the impact of the passive uptake Cl value on the overall *in vitro – in vivo* correlations between reported and predicted hepatic Cl of HIV PI (Figure 4). When the experimentally determined passive uptake Cl of each PI was relatively increased or decreased with a factor 2, only a

marginal effect on the correlation coefficient was observed. This suggests that up to 2-fold inaccuracies in passive diffusion estimates or moderate involvement of sinusoidal efflux transport would not substantially affect the conclusion regarding the rate-limiting role of hepatic uptake transporters in HIV PI disposition. In this context, it is noteworthy that nelfinavir has indeed been recently shown to be a substrate and inhibitor for the sinusoidal efflux transporter MRP4 (ABCC4).[41]

To further assess the impact of OATP1B inhibition or induction, the sensitivity of overall Cl predictions towards alterations in active hepatic uptake Cl was evaluated for each individual HIV PI (Figure 5). Our simulations revealed that decreased hepatic Cl can be expected for lopinavir, atazanavir and tipranavir upon potent inhibition of OATP1B-mediated transport Cl. These findings are in agreement with the increased plasma concentration of lopinavir in presence of the 521T>C gene polymorphism in *SLCO1B1*.[20] On the contrary, other HIV PI will most likely not be involved as victim drugs in drug – drug interactions mediated by OATP-mediated uptake inhibition. Furthermore, these data showed that induction of the OATP1B expression in hepatocytes may lead to an increased hepatic Cl of several HIV PI, contributing to variability in plasma concentrations of these drugs.

Results from PBPK modelling for three selected HIV protease inhibitors illustrate improved prediction of plasma concentrations when hepatic uptake data are included (Figure 6). The increase in predicted plasma concentrations upon switching from a perfusion-limited to a permeability-limited liver model is consistent with hepatic uptake transport being the rate-limiting step in hepatic elimination of these HIV protease inhibitors. However, the PBPK data also illustrate the necessity to determine other transporter-mediated processes for these HIV PI in human liver (e.g. sinusoidal efflux transport and biliary excretion). It should also be noted that

the substantial underprediction of amprenavir exposure may be due to auto-inhibition, as amprenavir has been reported to be both a competitive and mechanism-based inhibitor of CYP3A4/5.[42,43] However, several attempts to take this into account in the PBPK model did not lead to improved predictions: implementation of competitive inhibition had limited effect, while implementation of mechanism-based inhibition resulted in extremely slow elimination as compared to observed data. This suggests that other processes are also involved requiring further in vitro investigations.

In conclusion, these results illustrate that several HIV PI are transported *in vitro* by OATP1B1 and OATP1B3 isoforms in transfected cells. By combining the RAF method for determining active hepatic uptake Cl with estimates for passive uptake Cl, we revealed that hepatic uptake is the rate-limiting process in the overall hepatic Cl of several HIV PI. Therefore, potent inhibition or induction of transporter-mediated uptake of these drugs may significantly influence of plasma concentrations of some HIV PI.

AUTHORSHIP CONTRIBUTIONS

Participated in research design: De Bruyn, Augustijns, Annaert

Conducted experiments: De Bruyn

Contributed new reagents or analytic tools: Stieger, Augustijns, Annaert

Performed data analysis: De Bruyn, Annaert

Wrote or contributed to the writing of the manuscript: De Bruyn, Augustijns, Annaert

ACKNOWLEDGEMENTS

Tom De Bruyn received a PhD scholarship from the Agency for Innovation by Science and Technology, Flanders. This study was supported by grants from 'Fonds voor Wetenschappelijk Onderzoek', Flanders and 'Onderzoeksfonds' of the KU Leuven, Belgium.

REFERENCES

1. Ohtsuki S, Schaefer O, Kawakami H, Inoue T, Liehner S, Saito A, Ishiguro N, Kishimoto W, Ludwig-Schwellinger E, Ebner T, Terasaki T. 2012. Simultaneous absolute protein quantification of transporters, cytochromes P450, and UDP-glucuronosyltransferases as a novel approach for the characterization of individual human liver: comparison with mRNA levels and activities. Drug Metab. Dispos. 40:83–92.

2. Ieiri I, Higuchi S, Sugiyama Y. 2009. Genetic polymorphisms of uptake (OATP1B1, 1B3) and efflux (MRP2, BCRP) transporters: implications for inter-individual differences in the pharmacokinetics and pharmacodynamics of statins and other clinically relevant drugs. Expert Opin Drug Metab Toxicol 5:703–729.

3. König J. 2011. Uptake transporters of the human OATP family: molecular characteristics, substrates, their role in drug-drug interactions, and functional consequences of polymorphisms. Handb Exp Pharmacol 1–28.

4. Niemi M, Pasanen MK, Neuvonen PJ. 2011. Organic anion transporting polypeptide 1B1: a genetically polymorphic transporter of major importance for hepatic drug uptake. Pharmacol. Rev 63:157–181.

5. Thompson MA, Aberg JA, Cahn P, Montaner JSG, Rizzardini G, Telenti A, Gatell JM, Günthard HF, Hammer SM, Hirsch MS, Jacobsen DM, Reiss P, Richman DD, Volberding PA, Yeni P, Schooley RT. 2010. Antiretroviral Treatment of Adult HIV Infection. JAMA: The Journal of the American Medical Association 304:321 –333.

6. Hull MW, Montaner JSG. 2011. Ritonavir-boosted protease inhibitors in HIV therapy. Ann. Med. 43:375–388.

7. Vermeir M, Lachau-Durand S, Mannens G, Cuyckens F, van Hoof B, Raoof A. 2009. Absorption, Metabolism, and Excretion of Darunavir, a New Protease Inhibitor, Administered Alone and with Low-Dose Ritonavir in Healthy Subjects. Drug Metabolism and Disposition 37:809 –820.

8. Griffin L, Annaert P, Brouwer KLR. 2011. Influence of drug transport proteins on the pharmacokinetics and drug interactions of HIV protease inhibitors. J Pharm Sci 100:3636–3654.

9. Kis O, Robillard K, Chan GNY, Bendayan R. 2010. The complexities of antiretroviral drug-drug interactions: role of ABC and SLC transporters. Trends in Pharmacological Sciences 31:22–35.

10. Parker AJ, Houston JB. 2008. Rate-limiting steps in hepatic drug clearance: comparison of hepatocellular uptake and metabolism with microsomal metabolism of saquinavir, nelfinavir, and ritonavir. Drug Metab. Dispos 36:1375–1384.

11. Yabe Y, Galetin A, Houston JB. 2011. Kinetic characterization of rat hepatic uptake of 16 actively transported drugs. Drug Metab. Dispos. 39:1808–1814.

12. Lam JL, Okochi H, Huang Y, Benet LZ. 2006. In vitro and in vivo correlation of hepatic transporter effects on erythromycin metabolism: characterizing the importance of transporter-enzyme interplay. Drug Metab. Dispos 34:1336–1344.

13. Endres CJ, Endres MG, Unadkat JD. 2009. Interplay of drug metabolism and transport: a real phenomenon or an artifact of the site of measurement?. Mol. Pharm 6:1756–1765.

14. Annaert P, Ye ZW, Stieger B, Augustijns P. 2010. Interaction of HIV protease inhibitors with OATP1B1, 1B3, and 2B1. Xenobiotica 40:163–176.

15. De Bruyn T, Fattah S, Stieger B, Augustijns P, Annaert P. 2011. Sodium fluorescein is a probe substrate for hepatic drug transport mediated by OATP1B1 and OATP1B3. J Pharm Sci 100:5018–5030.

16. Campbell SD, de Morais SM, Xu JJ. 2004. Inhibition of human organic anion transporting polypeptide OATP 1B1 as a mechanism of drug-induced hyperbilirubinemia. Chemico-Biological Interactions 150:179–187.

17. Karlgren M, Ahlin G, Bergström CAS, Svensson R, Palm J, Artursson P. 2012. In vitro and in silico strategies to identify OATP1B1 inhibitors and predict clinical drug-drug interactions. Pharm. Res. 29:411–426.

18. Shitara Y. 2011. Clinical Importance of OATP1B1 and OATP1B3 in Drug-Drug Interactions. Drug Metab. Pharmacokinet 26:220–227.

19. Su Y, Zhang X, Sinko PJ. 2004. Human organic anion-transporting polypeptide OATP-A (SLC21A3) acts in concert with P-glycoprotein and multidrug resistance protein 2 in the vectorial transport of Saquinavir in Hep G2 cells. Mol. Pharm. 1:49–56.

20. Hartkoorn RC, Kwan WS, Shallcross V, Chaikan A, Liptrott N, Egan D, Sora ES, James CE, Gibbons S, Bray PG, Back DJ, Khoo SH, Owen A. 2010. HIV protease inhibitors are substrates for OATP1A2, OATP1B1 and OATP1B3 and lopinavir plasma concentrations are influenced by SLCO1B1 polymorphisms. Pharmacogenet. Genomics 20:112–120.

21. Lubomirov R, di Iulio J, Fayet A, Colombo S, Martinez R, Marzolini C, Furrer H, Vernazza P, Calmy A, Cavassini M, Ledergerber B, Rentsch K, Descombes P, Buclin T, Decosterd LA, Csajka C, Telenti A. 2010. ADME pharmacogenetics: investigation of the pharmacokinetics of the antiretroviral agent lopinavir coformulated with ritonavir. Pharmacogenet. Genomics 20:217–230.

22. Liu L, Unadkat JD. 2013. Interaction between HIV protease inhibitors (PIs) and hepatic transporters in sandwich cultured human hepatocytes: implication for PI-based DDIs. Biopharm Drug Dispos 34:155–164.

23. De Bruyn T, Ye Z-W, Peeters A, Sahi J, Baes M, Augustijns PF, Annaert PP. 2011. Determination of OATP-, NTCP- and OCT-mediated substrate uptake activities in individual and pooled batches of cryopreserved human hepatocytes. Eur J Pharm Sci 43:297–307.

24. Obach RS. 1999. Prediction of human clearance of twenty-nine drugs from hepatic microsomal intrinsic clearance data: An examination of in vitro half-life approach and nonspecific binding to microsomes. Drug Metab. Dispos. 27:1350–1359.

25. Kouzuki H, Suzuki H, Ito K, Ohashi R, Sugiyama Y. 1998. Contribution of Sodium Taurocholate Co-Transporting Polypeptide to the Uptake of Its Possible Substrates Into Rat Hepatocytes. J Pharmacol Exp Ther 286:1043–1050.

26. Hirano M, Maeda K, Shitara Y, Sugiyama Y. 2004. Contribution of OATP2 (OATP1B1) and OATP8 (OATP1B3) to the hepatic uptake of pitavastatin in humans. J. Pharmacol. Exp. Ther. 311:139–146.

27. Shimizu M, Fuse K, Okudaira K, Nishigaki R, Maeda K, Kusuhara H, Sugiyama Y. 2005. Contribution of OATP (organic anion-transporting polypeptide) family transporters to the hepatic uptake of fexofenadine in humans. Drug Metab. Dispos. 33:1477–1481.

28. Kitamura S, Maeda K, Wang Y, Sugiyama Y. 2008. Involvement of multiple transporters in the hepatobiliary transport of rosuvastatin. Drug Metab. Dispos. 36:2014–2023.

29. Seewöster T, Lehmann J. 1997. Cell size distribution as a parameter for the predetermination of exponential growth during repeated batch cultivation of CHO cells. Biotechnol. Bioeng. 55:793–797.

[30] H. Lodish, A. Berk, S. L. Zipursky, P. Matsudaira, D. Baltimore, J. Darnell. Molecular Cell Biology, W. H. Freeman, 2000.

31. Webborn PJH, Parker AJ, Denton RL, Riley RJ. 2007. In vitro-in vivo extrapolation of hepatic clearance involving active uptake: theoretical and experimental aspects. Xenobiotica 37:1090–1109.

32. Treiber A, Schneiter R, Häusler S, Stieger B. 2007. Bosentan is a substrate of human OATP1B1 and OATP1B3: inhibition of hepatic uptake as the common mechanism of its interactions with cyclosporin A, rifampicin, and sildenafil. Drug Metab. Dispos 35:1400–1407.

33. De Bruyn T, Van Westen GJP, Ijzerman AP, Stieger B, de Witte P, Augustijns PF, Annaert PP. 2013. Structure-based Identification of OATP1B1/3 Inhibitors. Mol. Pharmacol. 83:1257–67.

34. Dingemanse J, van Giersbergen PLM, Patat A, Nilsson PN. 2010. Mutual pharmacokinetic interactions between bosentan and lopinavir/ritonavir in healthy participants. Antivir. Ther. (Lond.) 15:157–163.

35. Kiser JJ, Gerber JG, Predhomme JA, Wolfe P, Flynn DM, Hoody DW. 2008. Drug/Drug interaction between lopinavir/ritonavir and rosuvastatin in healthy volunteers. J. Acquir. Immune Defic. Syndr. 47:570–578.

36. Riley RJ, McGinnity DF, Austin RP. 2005. A unified model for predicting human hepatic, metabolic clearance from in vitro intrinsic clearance data in hepatocytes and microsomes. Drug Metab. Dispos 33:1304–1311.

37. Decker CJ, Laitinen LM, Bridson GW, Raybuck SA, Tung RD, Chaturvedi PR. 1998. Metabolism of amprenavir in liver microsomes: role of CYP3A4 inhibition for drug interactions. J Pharm Sci 87:803–807.

38. Koudriakova T, Iatsimirskaia E, Utkin I, Gangl E, Vouros P, Storozhuk E, Orza D, Marinina J, Gerber N. 1998. Metabolism of the human immunodeficiency virus protease inhibitors indinavir and ritonavir by human intestinal microsomes and expressed cytochrome P4503A4/3A5: mechanism-based inactivation of cytochrome P4503A by ritonavir. Drug Metab. Dispos. 26:552–561.

39. Kumar GN, Dykstra J, Roberts EM, Jayanti VK, Hickman D, Uchic J, Yao Y, Surber B, Thomas S, Granneman GR. 1999. Potent inhibition of the cytochrome P-450 3A-mediated human liver microsomal metabolism of a novel HIV protease inhibitor by ritonavir: A positive drug-drug interaction. Drug Metab. Dispos. 27:902–908.

40. Wempe MF, Anderson PL. 2011. Atazanavir metabolism according to CYP3A5 status: an in vitro-in vivo assessment. Drug Metab. Dispos. 39:522–527.

41. Fukuda Y, Takenaka K, Sparreboom A, Cheepala SB, Wu C-P, Ekins S, Ambudkar SV, Schuetz JD. 2013. Human immunodeficiency virus protease inhibitors interact with ATP binding cassette transporter 4/multidrug resistance protein 4: a basis for unanticipated enhanced cytotoxicity. Mol. Pharmacol. 84:361–371.

42. Zimmerlin A, Trunzer M, Faller B. 2011. CYP3A time-dependent inhibition risk assessment validated with 400 reference drugs. Drug Metab. Dispos. 39:1039–1046.

43. Zhao P, Kunze KL, Lee CA. 2005. Evaluation of time-dependent inactivation of CYP3A in cryopreserved human hepatocytes. Drug Metab. Dispos. 33:853–861.

44. Sadler BM, Piliero PJ, Preston SL, Lloyd PP, Lou Y, Stein DS. 2001. Pharmacokinetics and safety of amprenavir and ritonavir following multiple-dose, co-administration to healthy volunteers. AIDS 15:1009–1018.

45. Swainston Harrison T, Scott LJ. 2005. Atazanavir: a review of its use in the management of HIV infection. Drugs 65:2309–2336.

46. Hughes CA, Robinson L, Tseng A, MacArthur RD. 2009. New antiretroviral drugs: a review of the efficacy, safety, pharmacokinetics, and resistance profile of tipranavir, darunavir, etravirine, rilpivirine, maraviroc, and raltegravir. Expert Opin Pharmacother 10:2445–2466.

47. Rittweger M, Arastéh K. 2007. Clinical pharmacokinetics of darunavir. Clin Pharmacokinet 46:739–756.

48. Plosker GL, Noble S. 1999. Indinavir: a review of its use in the management of HIV infection. Drugs 58:1165–1203.

49. Chandwani A, Shuter J. 2008. Lopinavir/ritonavir in the treatment of HIV-1 infection: a review. Ther Clin Risk Manag 4:1023–1033.

50. Perry CM, Frampton JE, McCormack PL, Siddiqui MAA, Cvetković RS. 2005. Nelfinavir: a review of its use in the management of HIV infection. Drugs 65:2209–2244.

51. Hsu A, Granneman GR, Bertz RJ. 1998. Ritonavir. Clinical pharmacokinetics and interactions with other anti-HIV agents. Clin Pharmacokinet 35:275–291.

52. Vella S, Floridia M. 1998. Saquinavir. Clinical pharmacology and efficacy. Clin Pharmacokinet 34:189–201.

53. Gui C, Miao Y, Thompson L, Wahlgren B, Mock M, Stieger B, Hagenbuch B. 2008. Effect of pregnane X receptor ligands on transport mediated by human OATP1B1 and OATP1B3. Eur. J. Pharmacol 584:57–65.

FIGURE LEGENDS

Supplemental Figure 1

Time-dependent uptake of tipranavir (panel A) and indinavir (panel B) by wild-type (circles), OATP1B1- (squares) and OATP1B3- (triangles) transfected CHO cells. CHO cells were incubated with 0.25 μM TPV and 2.5 μM IDV. Points represent mean (± SD) of triplicate determinations.

Figure 1

Uptake of HIV PI by OATP1B1- (black bars) and OATP1B3- (open bars) transfected CHO cells Bars represent mean (± SD) uptake ratios obtained by normalizing the uptake in transfected cells for the uptake in wild-type CHO cells. ** $p < 0.01$ and * $p < 0.05$ (two-tailed Student's t-test). Uptake (30 s) was determined at one clinically relevant test concentration; 1 μM for amprenavir, atazanavir and tipranavir; 2.5 μM for indinavir; 0.25 μM for lopinavir, nelfinavir, ritonavir, saquinavir and tipranavir.

Figure 2

Relationship between metabolic rate and tipranavir concentration in pooled (n = 45) human liver microsomes. Points represent means (± SD) of triplicate incubations and the solid line represents the best fit to experimental data according to the Michaelis-Menten equation.

Figure 3

Relationship between the reported and calculated hepatic Cl of all HIV PI. Calculated hepatic Cl was predicted based on *in vitro* uptake Cl data only (A), metabolic Cl data only (B) or a combination of both uptake and metabolic Cl data (C).

Figure 4

Simulation of the effect of the passive uptake Cl on the relationship between reported and calculated hepatic Cl of HIV PI. The predicted correlation coefficient of the relationship between reported and calculated hepatic Cl is expressed in function of the passive Cl (expressed as a percentage of the measured passive Cl).

Figure 5

Simulation of the effect on the hepatic Cl when active uptake is 90 % inhibited (open bars) or when active uptake is 5-fold induced (grey bars) in function of control condition.

Figure 6

Observed (points) and predicted (lines) plasma concentration time profiles for darunavir, atazanavir and amprenavir. Predictions were generated based on PBPK models in the Simcyp simulator v.14. Left and right panels represent predictions for perfusion-limited and permeability-limited liver models. All other parameters were kept fixed between both models.

Table 1

Comparison of the experimental concentrations used in the present study to the reported maximum unbound peak plasma concentrations of HIV PI.

Substrate	*In vitro* concentration (μM) (present study)	fu	Unbound peak plasma concentrations (μM) (reported)	Reference
Amprenavir	1	0.1	1 – 3.2	[44]
Atazanavir	1	0.14	0.6 – 1.3	[45]
Darunavir	1	0.07	0.3 – 1.1	[46,47]
Indinavir	2.5	0.35	1.7 – 4.4	[48]
Lopinavir	0.25	0.02	0.3	[49]
Nelfinavir	0.25	0.02	0.1	[50]
Ritonavir	0.25	0.01	0.16	[51]
Saquinavir	0.25	0.02	0.11 – 0.3	[52]
Tipranavir	0.25	0.001	0.06 – 0.19	[46]

Table 2

Transitions monitored, optimized parameters and retention time for LC-MS/MS analysis.

Substrate	Transition	CT	VT	SG	AG	ISG	CE	RT (min)
Darunavir	548.3 → 392.3	275	300	30	5	20	12	2.7
Atazanavir	705.4 → 168.1	170	300	50	0	40	43	3.16
Lopinavir	629.4 → 155.2	170	300	50	0	40	38	3.4
Saquinavir	671.5 → 570.4	275	300	60	55	10	29	3.25
Ritonavir	721.3 →140.0	220	300	60	10	25	57	3.19
	721.3 →197.0						35	
	721.3 →268.1						24	
	721.3 →296.0						16	
Tipranavir	603.3 → 411.1	280	300	60	0	10	21	3.34
	603.3 → 585.4						14	
Nelfinavir	568.3 → 330.1	275	300	50	10	10	30	3.3
Indinavir	614.5 → 421.3	275	300	50	5	10	32	2.94
Amprenavir	506.3 → 245.2	270	300	60	2	30	17	2.68

CT, capillary temperature; VT, vaporizing temperature; SG, sheet gas; AG, auxiliary gas; ISG, ion sweep gas; CE, collision energy; RT, retention time

Table 1

Comparison of the experimental concentrations used in the present study to the reported maximum unbound peak plasma concentrations of HIV PI.

Substrate	*In vitro* concentration (μM) (present study)	fu	Unbound peak plasma concentrations (μM) (reported)	Reference
Amprenavir	1	0.1	1 – 3.2	[44]
Atazanavir	1	0.14	0.6 – 1.3	[45]
Darunavir	1	0.07	0.3 – 1.1	[46,47]
Indinavir	2.5	0.35	1.7 – 4.4	[48]
Lopinavir	0.25	0.02	0.3	[49]
Nelfinavir	0.25	0.02	0.1	[50]
Ritonavir	0.25	0.01	0.16	[51]
Saquinavir	0.25	0.02	0.11 – 0.3	[52]
Tipranavir	0.25	0.001	0.06 – 0.19	[46]

Table 3: Physicochemical parameters and reported or experimentally determined *in vitro* drug disposition data used as input parameters for Simcyp simulations.

	Amprenavir	Atazanavir	Darunavir
Physicochemical parameters			
Log P	2.43	4.5	1.8
pK_a (basic)	2.39	4.42 / 1.37	2.39
B/P	1.99	1.09	0.7
fu	0.1	0.14	0.07
Absorption			
passive Caco-2 P_{app} (10^{-6} cm/s)	38	25	30
predicted $P_{eff\ man}$ (10^{-4} cm/s)	2.416	1.724	1.997
predicted fu_{gut}	0.030	0.00027	0.117
Q gut (predicted)	9.98	8.37	9.07
Distribution			
Vd (L/kg; *predicted with Method 2*)	6.140	1.550	1.259
Scalar	5.5841	0.00657	5.3671
Elimination			
Enzyme kinetics (CYP3A4)			
Vmax (pmol/min/mg microsomal protein)	287	138	157
Km (μM)	0.355	0.362	0.159
fu_{mic}	0.8	0.71	0.56
Cl_{renal} (L/h)	0.22	0.9	0.39
Transport			
Intestine			
ABCB1 (P-gp; $Cl_{int,t}$; μl/min)	0.18	0.18	0.42
Liver			
CL_{PD} (mL/min/10^6 hep)	0.0855	0.0043	0.0084
Sinus. uptake (μl/min/10^6 cells)			
OATP1B1	-	6.3	2.87
OATP1B3	-	0.3	0.89
Canalicular efflux (μl/min/10^6 cells)			
ABCB1 (P-gp)	-	0.401	0.18

Table 4

Uptake Cl of reference compounds (estrone-3-sulfate for OATP1B1 and CGamF for OATP1B3) in pooled human hepatocytes and OATP1B1- and OATP1B3-transfected CHO cells. The ratio of the uptake Cl of these reference compounds in human hepatocytes to that in transfected CHO cells is defined as the relative activity factor (RAF).

	estrone-3-sulfate	CGamF
Cl_{hep} (µl/min/million cells)	99.1[23]	14.8
$Cl_{OATP1B1}$ (µl/min/mg protein)	141.7[53]	(7.8)[14]
$Cl_{OATP1B3}$ (µl/min/mg protein)	(32)	142[14]
$RAF_{OATP1B1}$	0.70	N.D.
$RAF_{OATP1B3}$	N.D.	0.11

N.D. not determined

Table 5

Uptake Cl values of HIV PI measured in OATP1B1- and OATP1B3-transfected cells and predicted in human hepatocytes based on relative activity factor.

	Uptake Cl in transfected CHO cells (µl/min/mg protein)			Predicted uptake Cl in human hepatocytes
Compound	WT	OATP1B1	OATP1B3	(µl/min/million cells)
Darunavir	8.4	4.1	8.0	12.1
Atazanavir	4.3	9.0	2.8	10.9
Lopinavir	31.5	68.5	7.6	80.2
Saquinavir	155.4	51.0	34.9	194.7
Ritonavir	37.7	18.2	31.8	53.7
Tipranavir	119.0	168.1	236.4	261.5
Nelfinavir	285.8	113.3	174.3	383.4
Indinavir	7.9	5.0	9.8	12.4
Amprenavir	85.5	0	0	85.5

Table 6

In vitro metabolic Cl of all HIV PI determined in pooled (n = 45) liver microsomes.

Substrate	Km (nM)	Vmax (pmol/min/mg protein)	$Cl_{int, met}$ (ml/min/mg protein)	$Cl_{int, met} / f_{u, mic}$ (ml/min/mg protein)
Darunavir	159	157	0.99	1.76
Atazanavir	362	138	0.38	0.54
Lopinavir	879	3879	4.4	4.82
Saquinavir	288	1238	4.3	7.36
Ritonavir	325	61.0	0.17	0.22
Tipranavir	437	833	1.91	2.77
Nelfinavir	340	334	0.98	7.59
Indinavir	124	119	0.42	0.51
Amprenavir	355	287	0.81	1.01

Figure 1

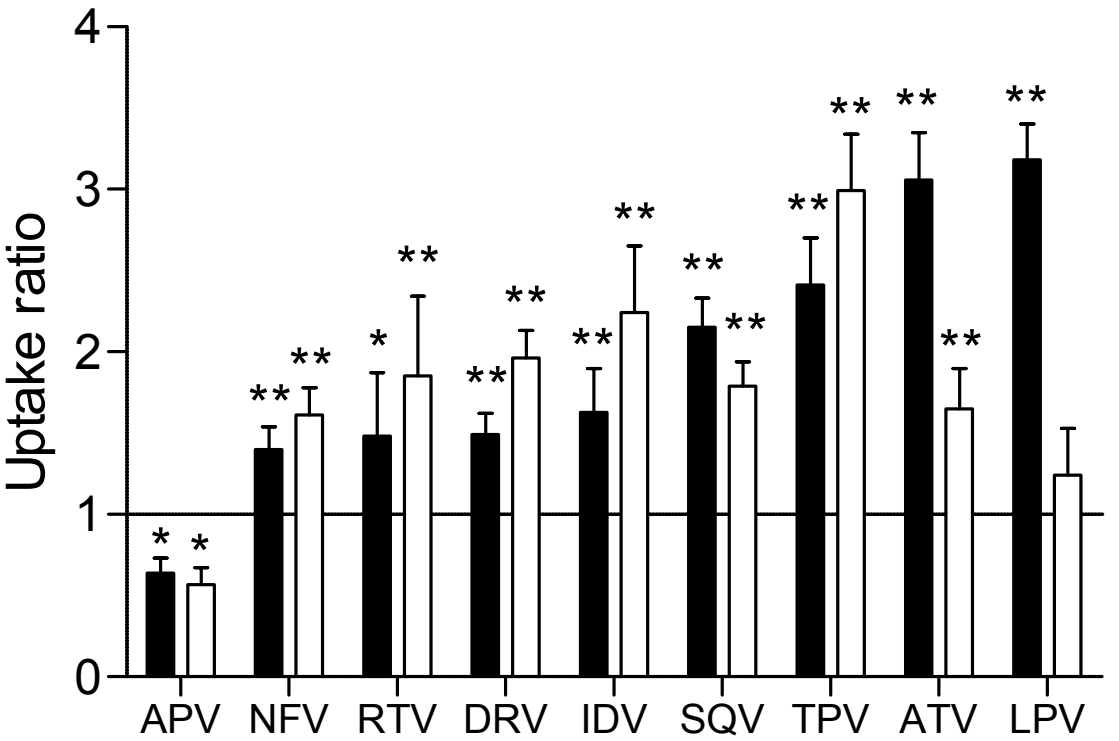

Figure 2

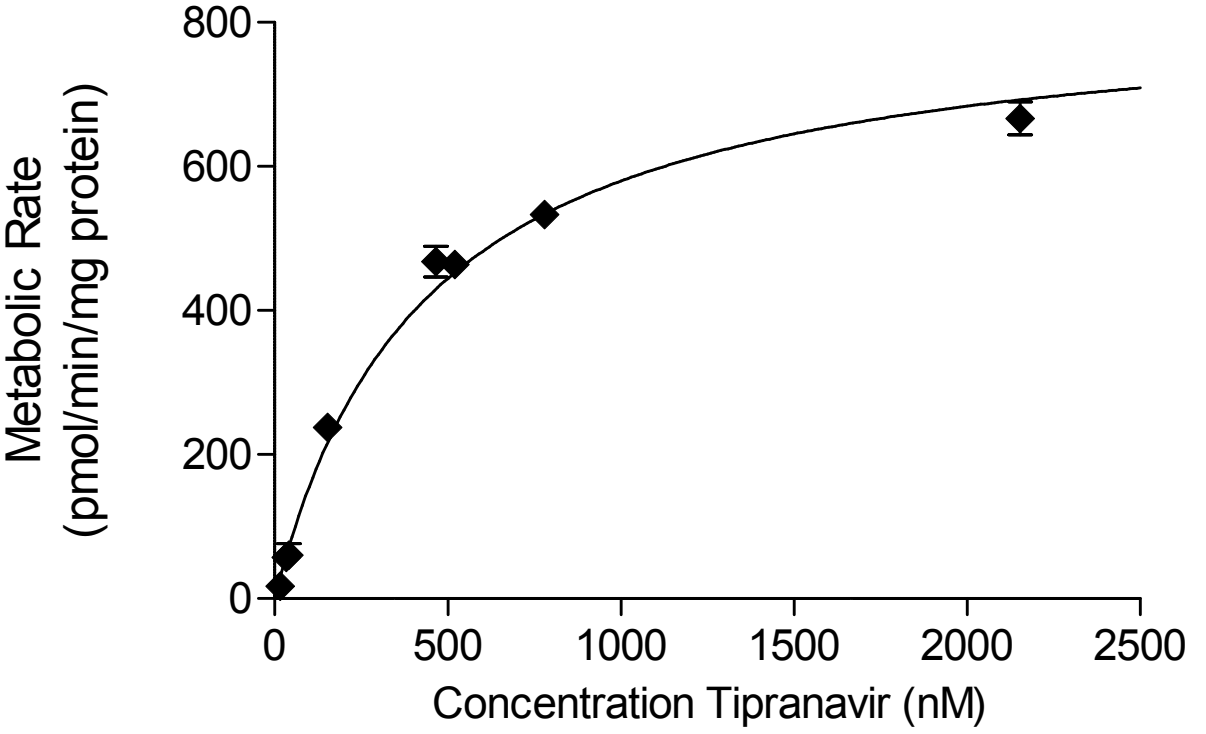
Metabolic Rate
(pmol/min/mg protein)
800
600
400
200
0
0
500
1000
1500
2000
2500
Concentration Tipranavir (nM)

Figure 3

A

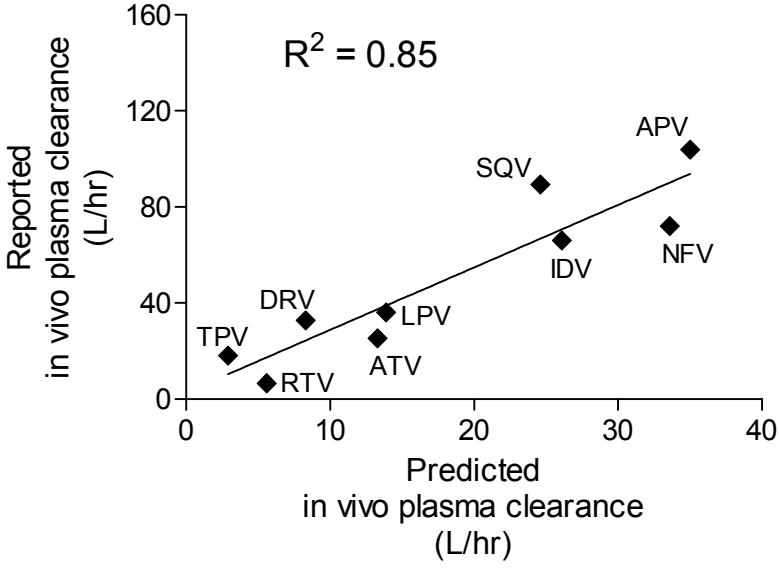
R^2 = 0.85
Reported in vivo plasma clearance (L/hr)
Predicted in vivo plasma clearance (L/hr)
APV
SQV
IDV
NFV
DRV
LPV
TPV
ATV
RTV
0
40
80
120
160
0
10
20
30
40

B

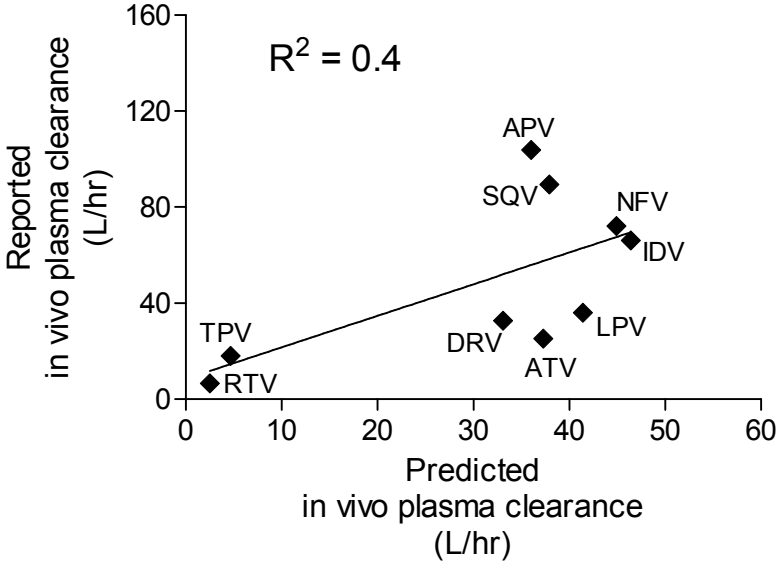
R^2 = 0.4
Reported in vivo plasma clearance (L/hr)
Predicted in vivo plasma clearance (L/hr)
APV
SQV
NFV
IDV
TPV
DRV
LPV
ATV
RTV
0
40
80
120
160
0
10
20
30
40
50
60

C

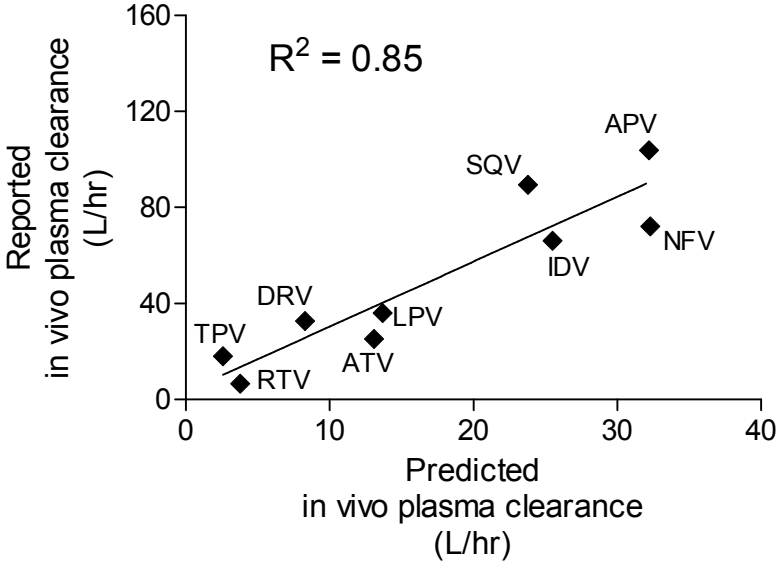
R^2 = 0.85
Reported in vivo plasma clearance (L/hr)
Predicted in vivo plasma clearance (L/hr)
APV
SQV
NFV
IDV
DRV
LPV
TPV
ATV
RTV
0
40
80
120
160
0
10
20
30
40

Figure 4

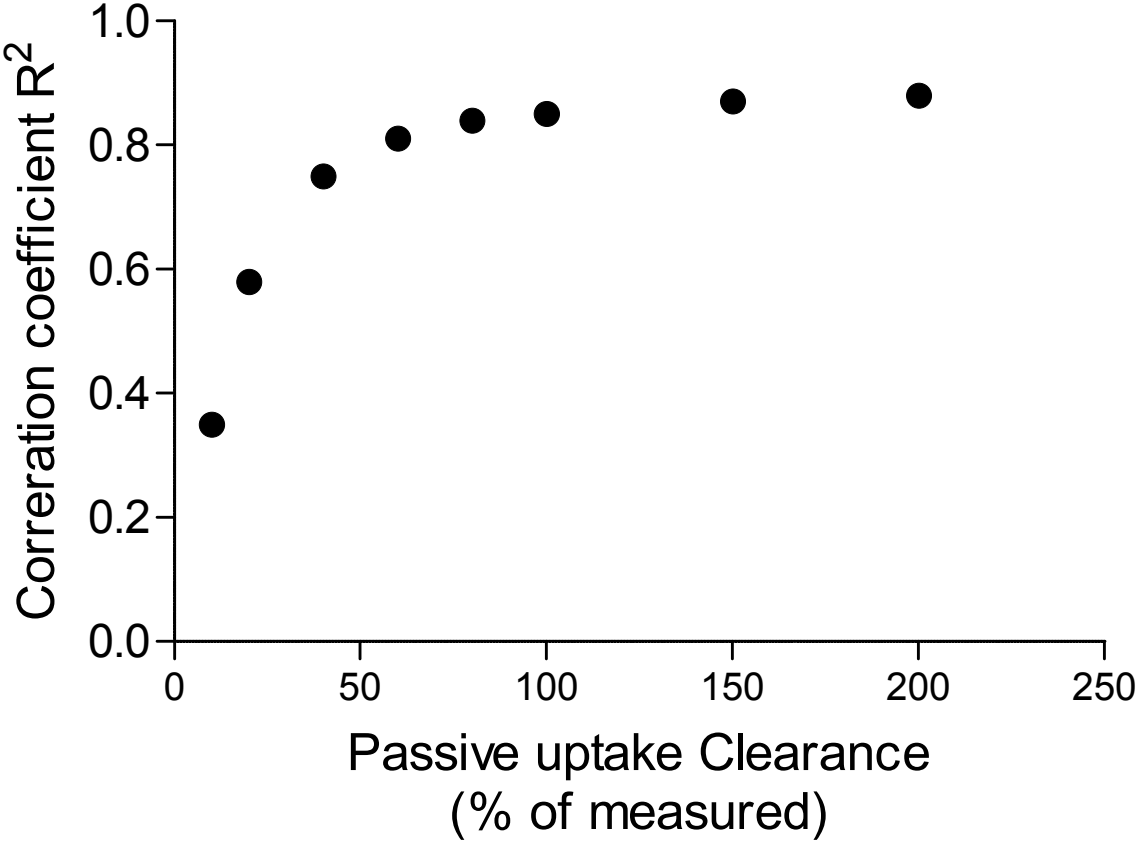
Correration coefficient R^2
1.0
0.8
0.6
0.4
0.2
0.0
0
50
100
150
200
250
Passive uptake Clearance
(% of measured)

Figure 5

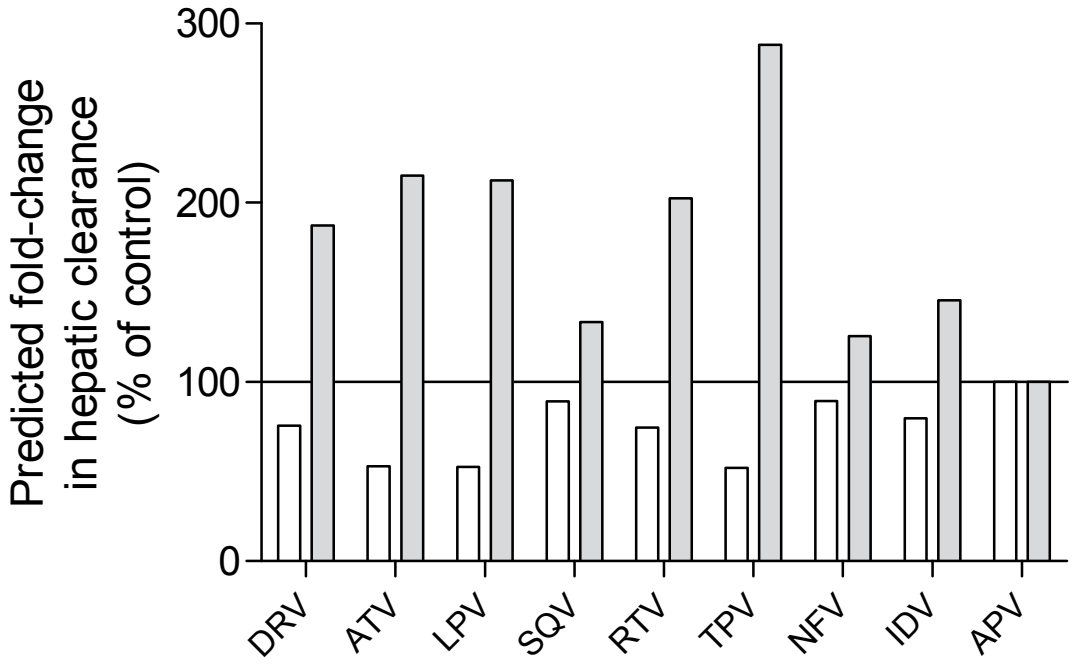
Predicted fold-change
in hepatic clearance
(% of control)
300
200
100
0
DRV
ATV
LPV
SQV
RTV
TPV
NFV
IDV
APV

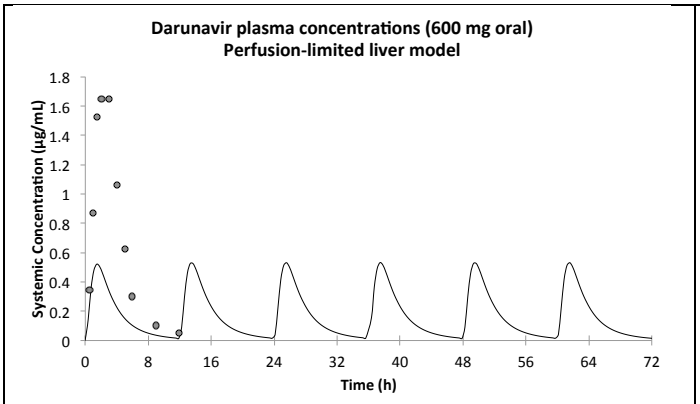
Darunavir plasma concentrations (600 mg oral)
Perfusion-limited liver model
Systemic Concentration (µg/mL)
Time (h)

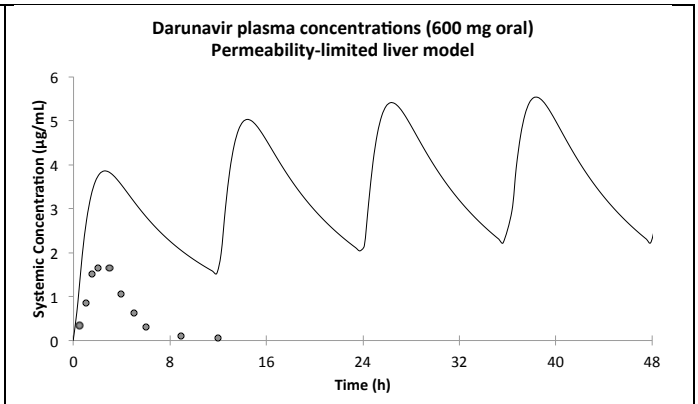
Darunavir plasma concentrations (600 mg oral)
Permeability-limited liver model
Systemic Concentration (µg/mL)
Time (h)

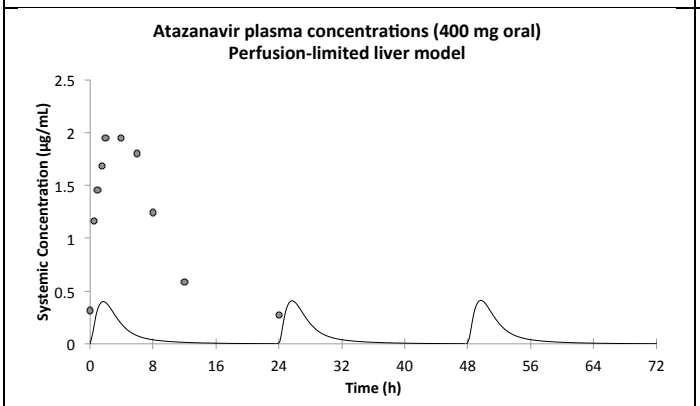
Atazanavir plasma concentrations (400 mg oral)
Perfusion-limited liver model
Systemic Concentration (µg/mL)
Time (h)

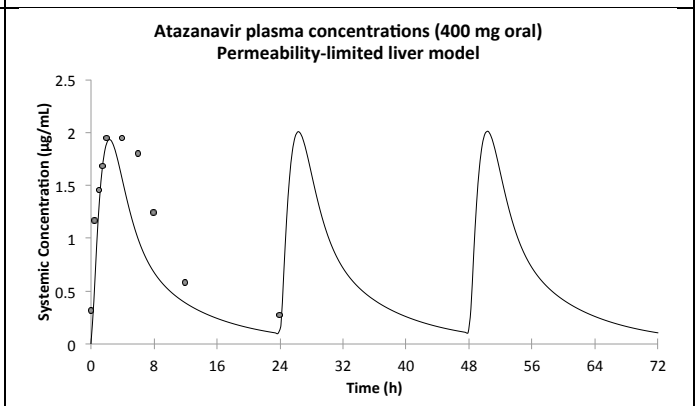
Atazanavir plasma concentrations (400 mg oral)
Permeability-limited liver model
Systemic Concentration (µg/mL)
Time (h)

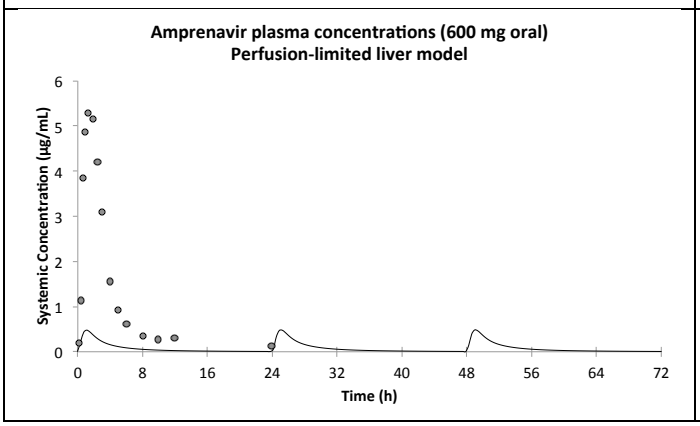
Amprenavir plasma concentrations (600 mg oral)
Perfusion-limited liver model
Systemic Concentration (µg/mL)
Time (h)

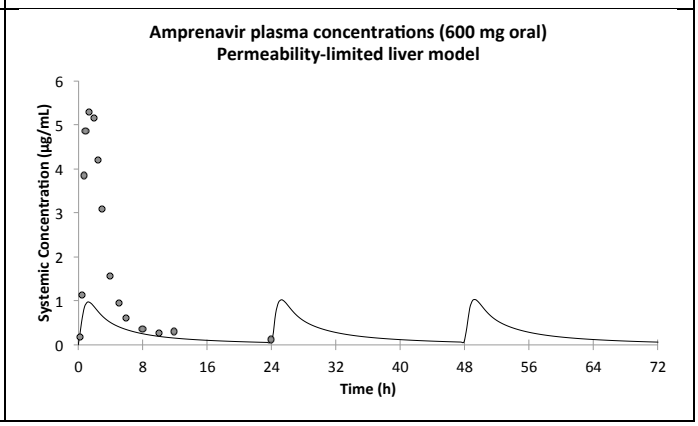
Amprenavir plasma concentrations (600 mg oral)
Permeability-limited liver model
Systemic Concentration (µg/mL)
Time (h)

Figure 1

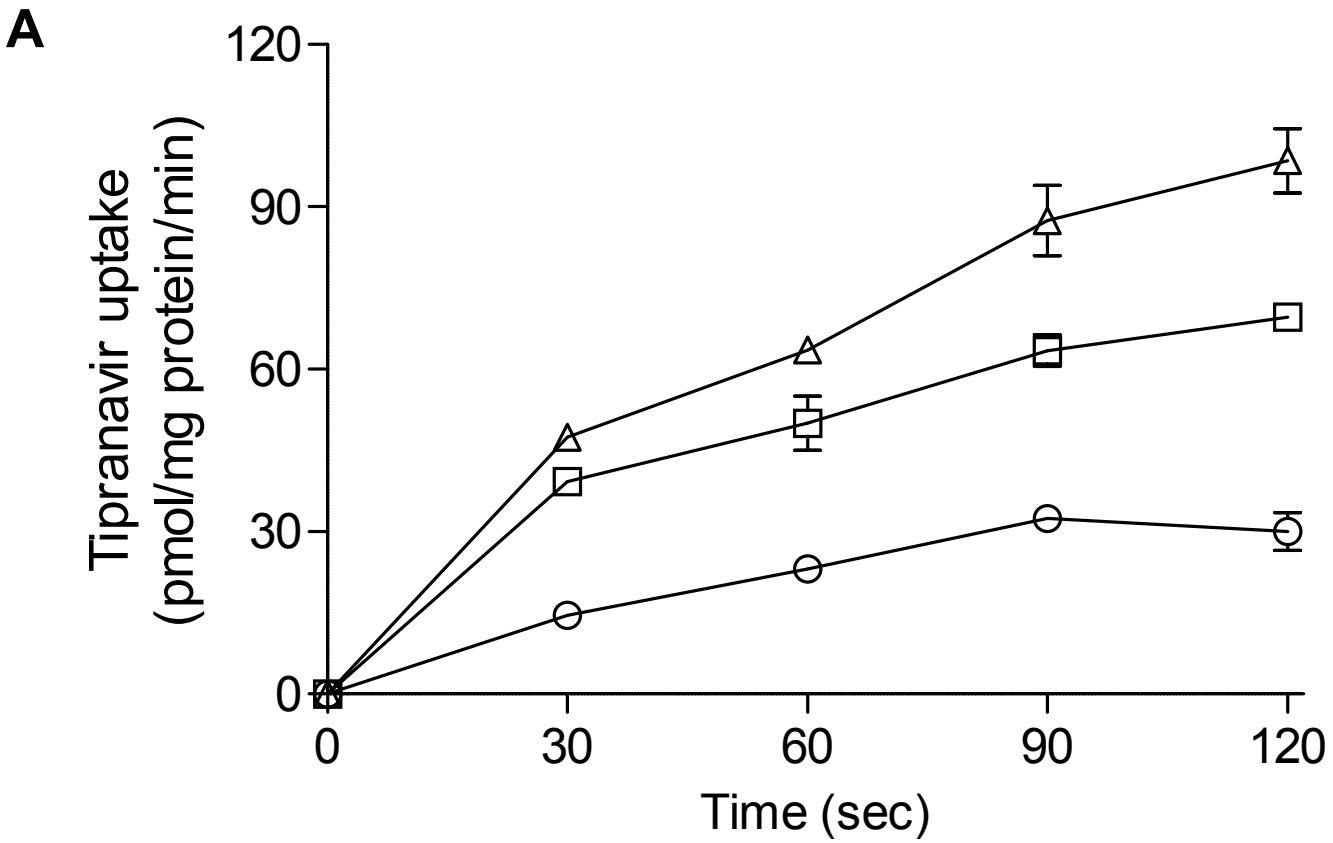
A
Tipranavir uptake
(pmol/mg protein/min)
120
90
60
30
0
0
30
60
90
120
Time (sec)

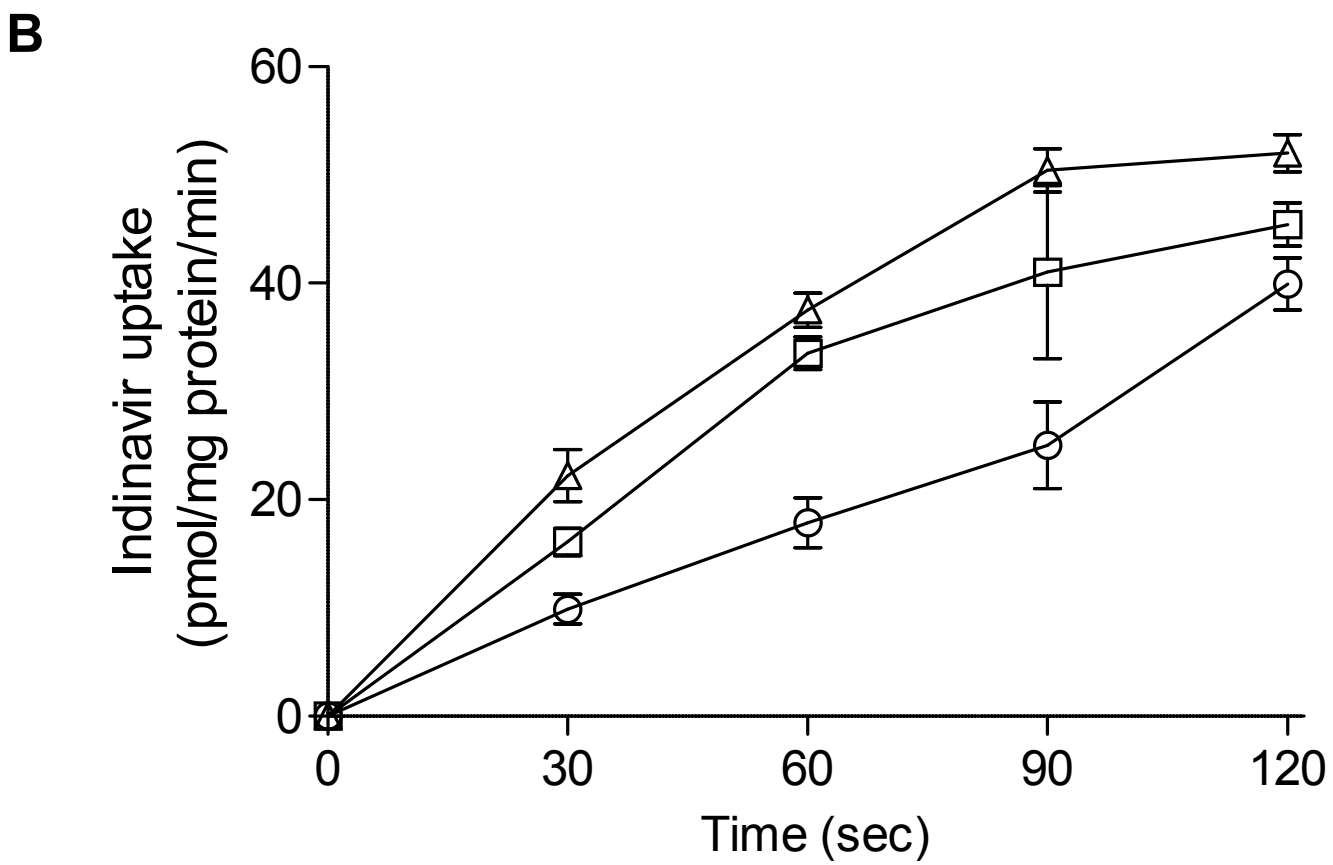
B
Indinavir uptake
(pmol/mg protein/min)
60
40
20
0
0
30
60
90
120
Time (sec)